Mausam, (1985), **36**, 1, 21-32

551.526.6 : 551.553.21

Surface heat budget estimates at selected areas of north Indian Ocean during Monsoon-77*

R. R. RAO, K. V. S. RAMAM, D. S. RAO and M. X. JOSEPH

Naval Physical & Oceanographic Laboratory, Cochin

(Received 16 October 1979)

सार — मानसून-77 के दौरान सोवियत रूस के चार स्थाई जहाजी बेड़ों से संग्रहीत समुद्री सतह के मौसम विज्ञानी और सूर्य-विकिरण आंकड़ों का भूतल वायुमण्डलीय सतह अभिलक्षणों के दिक्कालानुसार परिवर्तनों तथा उत्तरी हिन्द महासागर के कुछ चुनिन्दा क्षेत्रों में महासागरीय ताप बजट घटकों के निर्धारण के लिये उपयोग किया गया है । ग्रीष्मकालीन मानसून के शुरु होने और उसके विकसित होने के दौरान ताप बजट अवयवों की विशेषताओं में महत्वपूर्ण अन्तर दृष्टिगोचर हुए हैं । मानसूनी प्रवाह को समुद्रतल से प्रदत्त ऊर्जा में स्थानानुसार असमांगता दर्शाई गई है । दृष्टव्य है कि खराब मौसम में समुद्र से जो ऊर्जा वायुमण्डल को प्राप्त होती है, वह ठीक मौसम में समुद्र से वायुमण्डलीय को मिलने वाली ऊर्जा से लगभग दुगनी होती है ।

ABSTRACT. Surface marine meteorological and solar radiation data collected during Monsoon-77 from USSR four ship stationary polygons are made use of to describe the space-time variability of surface atmospheric layer characteristics and the ocean surface heat budget components at selected areas of north Indian Ocean. Significant differences in the characteristics of heat budget components during the onset and progress of summer monsoon are noticed. Spatial non-homogeneity in the energy feed to the monsoonal flow from the ocean surface is highlighted. Energy input to the atmosphere from ocean during disturbed weather is found to be approximately double the corresponding value during fair weather period.

1. Introduction

Attempts are in rapid progress to understand the complex interactive role of Indian Ocean with the Indian summer monsoon. Bhumralker (1974) using IIOE data concluded that air-sea exchanges over the sea do not control the fluctuations of the monsoon but are themselves influenced by variation in intensity of the monsoonal flow. Pant (1977) using ISMEX-73 data reported that sensible heat flux shows a marked increase during disturbed period while the latent heat flux shows a decrease during the same period. Garstang (1967) reported that over limited regions of disturbances latent and sensible heat transfers are found to increase by an order of magnitude and when integrated over the whole disturbance the energy flux is found to be double the undisturbed value. Ramanadham *et al.* (1981) using Monsoon-77 data found that the latent heat flux associated with the onset vortex over Arabian Sea is larger than that associated with a depression over north Bay of Bengal. Based on time series data collected at two ships located in the off shore quasi-permanent trough region along the west coast of India during Monsoon-77 experiment, Rao *et al.* (1981) found that greater evaporation has occurred before the onset of monsoon as the air is relatively dry compared to the monsoon period, and after the complete onset of monsoon there is a decrease in evaporation by 30 to 40 per cent. The present study documents some of the properties of surface marine boundary layer and the surface heat budget estimates based on the observed marine meteorological and solar radiation data from the USSR four ship polygons over selected areas of north Indian Ocean during Monsoon-77.

2. Data

Hourly values of incoming solar radiation, albedo and surface marine meteorological data collected from four USSR ships during Monsoon-77 experiment are made use of in the present study. As the long wave radiation data coverage during day time is sparce, the values are estimated indirectly using empirical equations. Based on the hourly direct radiation and albedo values, the actual amounts of radiation available at the sea surface are estimated by integrating the hourly values from sunrise to sunset to obtain the daily totals. Parameters such as sea surface temperature (SST), atmospheric pressure, wind speed, low and total cloudiness, dry bulb and dew point temperatures are used to estimate latent heat and sensible heat exchanges with the aid of the bulk aerodynamic equations. Though, lot of uncertainty prevails in the accuracy of exchange coefficients, in the present investigation these

*This paper was presented in the symposium on "Monsoon Prediction" held at Indian Institute of Technology, New Delhi on 17 & 18 March 1979.

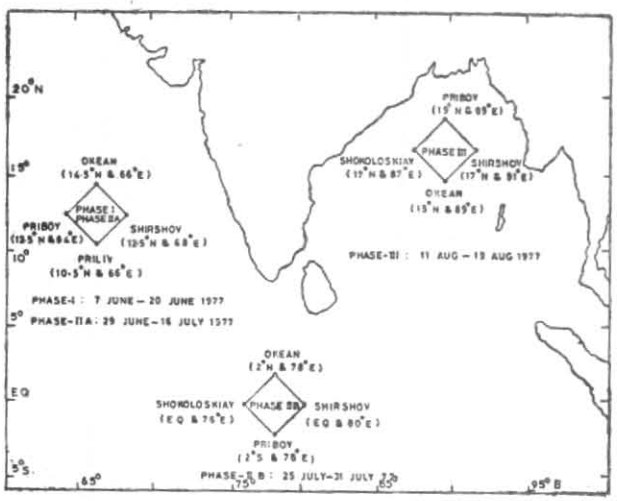

Fig. 1. Locations of stationary USSR ship polygon

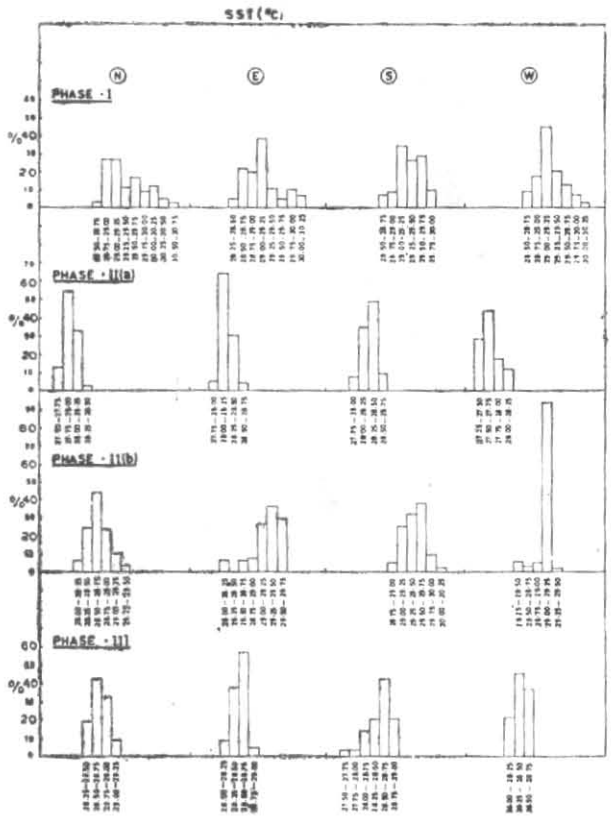

Fig. 2. Percentage frequency distribution of SST

coefficients are computed by the method proposed by Kondo (1975). The locations of the stationary USSR ship polygons are shown in Fig. 1 for all the three phases along with the periods of deployment. The four corners of the polygon in the clockwise from north are designated as N, E, S and W in the following discussion.

3. Methodology

Let Q represent the net heat gain at the surface which is the difference between the radiational input, *i.e.*, net radiation (Q_N) and heat losses, *viz.*, latent heat flux (Q_E) and sensible heat flux (Q_S) after neglecting other minor energy sources and sinks.

$$Q = Q_N - (Q_E + Q_S)$$

$$Q_N = Q_I - Q_B$$

$$Q_I = Q_D\,(1 - \alpha)$$

$$Q_B = \epsilon\sigma\, T_s^4\,(0.254 - 0.00495\, e)\, K$$

where,

Q_D : insolation impinging the sea surface

α : albedo of the sea surface

Q_I : available insolation at the sea surface after reflection

Q_B : net longwave radiation

ϵ : emissivity of the sea surface (.97)

σ : Steffan Boltzman constant $(0.813 \times 10^{-10}$ cal cm^{-2} K^{-4}min$^{-1})$

T_s : sea surface temperature (°K)

e : atmospheric vapour pressure (mb)

K : correction factor for cloudiness

Reed (1976) examined net longwave radiation data over oceanic surface in the light of various empirical formulae for estimating the irradiance. The observations suggest that Epimovas formula is the most realistic one for computing net longwave radiation under clear skies. Leavastu & Ayers (1966) have earlier suggested the values of K for cloud correction as :

$$K_L = (1.0 - 0.085\, C_L)$$
$$K_M = (1.0 - 0.065\, C_M)$$
$$K_H = (1.0 - 0.030\, C_H)$$

where C_L, C_M and C_H are respectively the low, medium and high clouds in tenths. On the advise of Kondo (1978) we have made the following assumptions to estimate medium and high clouds from the available total and low cloud values.

$$C_M = (C_T - C_L)/2$$
$$C_H = C_M$$

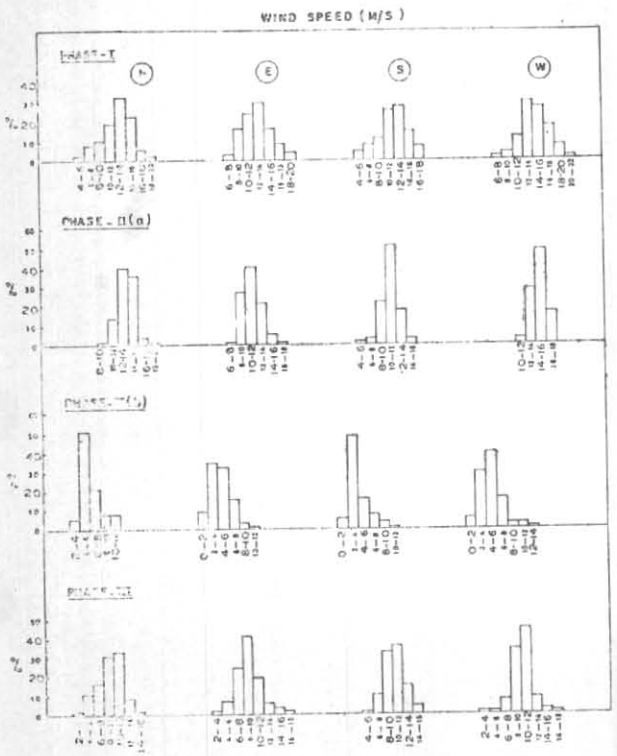

Fig. 3. Percentage frequency distribution of wind speed

where, C_T is the total cloudiness.

Using the values of K_L, K_M and K_H the value of K is calculated as,

$$K = (K_L + K_M + K_H) / 3$$

The net longwave radiation values obtained at hourly intervals are integrated for daily totals. The heat exchanges are estimated following bulk aerodynamic equations :

$$Q_E = \rho\, L\, C_{ED}\, (q_s - q_a)\, V$$
$$Q_S = \rho\, c_p\, C_{HD}\, (T_s - T_a)\, V$$

where,

ρ : density of the air (1.175×10^{-3} gm/cc)

L : latent heat of vaporisation (597 cal/gm)

V : wind speed (cm/sec)

c_p : the specific heat at constant pressure (0.24 cal/gm/°K)

T_a : dry bulb temperature (°K)

q_s and q_a : saturated specific humidities at sea surface temperature and dew point temperature respectively (gm/gm)

C_{ED} and C_{HD} : exchange coefficients of latent and sensible heat transfers evaluated using Kondo's (1975) method.

Murray's (1967) formula is used to estimate the saturation vapour pressure at SST and dew point temperature for the humidity mixing ratio gradient. The terms net 'heat gain' and 'heat loss' used in the discussion refers to oceanic medium being positive and negative respectively.

4. Analysis and discussion

Percentage frequency distribution of the basic parameters such as sea surface temperature, wind speed, and vapour pressure gradient are presented to indicate the fluctuatory nature of the marine boundary layer under different regimes of the monsoon.

Fig. 2 shows the percentage frequency distribution of SST for all the phases at the four locations of the USSR polygon. The large variance during Phase I may be attributed to the transient onset conditions of southwest monsoon over Arabian Sea. At all the locations the temperature interval for the highest frequency is 29.00 to 29.25 deg. C. The average values of the entire Phase I are greater than 29.0 deg. C (*see* Tables 1 a & b). During Phase II A the entire spectrum shifted towards lower side clearly indicating marked fall in SST at all the locations with the maximum shift at W location. The fall of SST may be accounted by loss of energy through evaporation, entrainment of colder waters below mixed layer due to convective and mechanical mixing and advection of colder waters upwelled off Somali coast. Another noteworthy feature is the low variance in SST when the monsoon is under full sway. But the temperature interval corresponding to the maximum frequency is no more same for all the locations indicating a meso scale variability within the polygon in the air-sea interface processes of the monsoon regime. During Phase IIA the percentage of occurrence of the values greater than 29.0 deg. C is zero at all the locations. During Phase IIB over equatorial Indian Ocean the scatter is minimum at the W location and is of similar order at the other three locations. The temperature interval corresponding to the maximum frequency is not same for all the locations. There is 1.0 deg. C difference between the S and N locations corresponding to the maximum frequency. The N location as a cooler area is quite conspicuous. Over northern Bay of Bengal during Phase III the maximum frequency corresponds to the interval for 28.50 to 28.75 deg. C at all the locations excepting the W location. The percentage of occurrence of the values greater than 28.5 deg. C indicates that N location is warmer than the other three.

TABLE 1 (a)

Averages of surface marine meteorological parameters and heat budget components of east central Arabian Sea

Parameter	Phase I					Phase IIA				
	N	E	S	W	Average	N	E	S	W	Average
SST (°C)	29.4	29.0	29.3	29.2	29.2	27.9	28.2	28.3	27.6	28.0
SMA (°C)	0.4	0.7	0.6	0.3	0.5	0.7	0.1	0.1	0.1	0.3
VPG (mb)	9.4	9.5	10.2	9.9	9.8	7.3	8.0	8.0	7.4	7.7
V (m/s)	11.9	12.1	11.3	13.8	12.3	13.1	10.7	10.3	14.1	12.0
$C_{ED} \times 10^3$	1.40	1.37	1.33	1.33	1.37	1.48	1.37	1.37	1.44	1.42
$C_{HD} \times 10^3$	1.39	1.35	1.30	1.36	1.35	1.48	1.35	1.36	1.43	1.41
Q_I (cal/cm²/day)	324	289	380	392	346	409	470	504	486	467
Q_B ,,	—75	—77	—81	—79	—78	—81	—82	—83	—85	—83
Q_N ,,	249	212	299	313	268	328	388	421	401	385
Q_E ,,	—614	—512	—605	—735	—542	—567	—460	—440	—586	—516
Q_S ,,	—13	—29	—23	—13	—20	—36	—3	—3	—5	—12
Q ,,	—378	—429	—329	—435	—393	—275	—75	—22	—190	—141
E (cm/day)	1.03	1.02	1.01	1.23	1.07	0.95	0.77	0.74	0.98	0.86
B	0.02	0.04	0.04	0.02	0.03	0.06	0.00	0.00	0.01	0.02

TABLE 1 (b)

Averages of surface marine meteorological parameters and heat budget components of equatorial Indian Ocean & north Bay of Bengal

Parameter	Phase IIB					Phase III				
	N	E	S	W	Average	N	E	S	W	Average
SST (°C)	28.6	29.3	29.4	29.0	29.1	28.7	28.4	28.5	28.4	28.5
SMA (°C)	0.3	1.1	1.6	1.0	1.0	0.3	0.6	0.2	0.2	0.3
VPG (mb)	9.1	11.6	12.0	8.0	10.2	5.6	6.6	6.1	5.6	6.0
V (m/s)	5.7	3.8	3.7	4.3	4.4	8.8	8.6	9.8	9.8	9.3
$C_{ED} \times 10^3$	1.30	1.42	1.44	1.33	1.37	1.33	1.33	1.35	1.34	1.34
$C_{HD} \times 10^3$	1.27	1.38	1.40	1.29	1.34	1.30	1.31	1.33	1.31	1.31
Q (cal/cm²/day)	526	466	410	389	448	312	427	397	465	400
Q_B ,,	—88	—89	—89	—75	—85	—69	—73	—73	—70	—71
Q_N ,,	438	377	321	314	463	243	354	324	295	304
Q_E ,,	—262	—227	—238	—181	—227	—249	—291	—318	—283	—285
Q_S ,,	—5	—16	—21	—16	—15	—8	—19	—9	—7	—11
Q ,,	171	134	62	117	121	—14	44	—3	5	8
E (cm/day)	0.44	0.38	0.40	0.30	0.38	0.42	0.49	0.53	0.47	0.48
B	0.02	0.06	0.08	0.07	0.07	0.03	0.05	0.02	0.02	0.03

E : Evaporation B : Bowen's Ratio

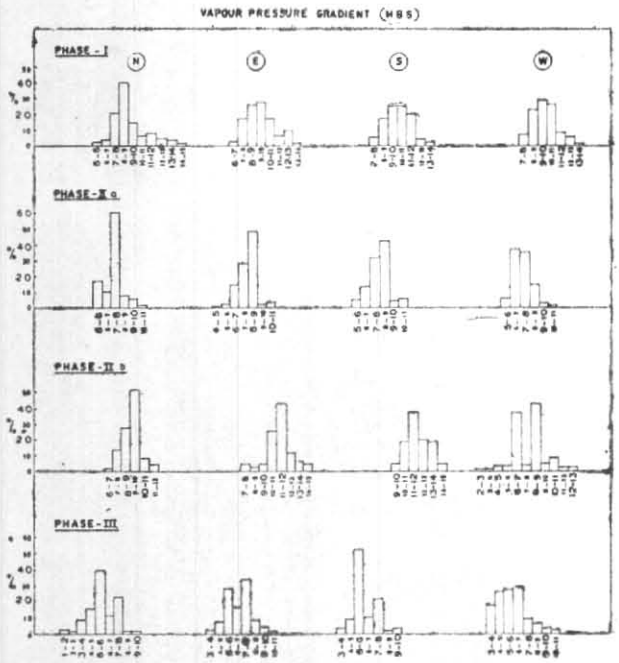

Fig. 4. Frequency distribution of vapour pressure gradient

Fig. 3 depicts the percentage frequency distribution of wind speed at all the four locations for all the phases. During Phase I the pattern is quite similar with maximum frequency occurring for 12 to 14 m/s interval at all the locations. The spread is more during Phase I compared to that of Phase IIA. Compared to Phase I, during Phase IIA there is an increase in the wind speed at N and W locations while there is a fall at E and S locations for the intervals corresponding to maximum frequency. This pattern can also be seen from the mean values of the two phases (*see* Tables 1 a & b). The change from Phase I to Phase IIA indicates that the wind field slightly weakened over southeast limb and strengthened over northwest limb of the polygon. Over equatorial Indian Ocean during Phase IIB the wind speeds are much weaker compared to Arabian Sea winds. The maximum frequency corresponds to 4-6 m/s at N & W locations and 2-4 m/s at E & S locations. Over Bay of Bengal during Phase III, the maximum frequency corresponds to 10-12 m/s for all the locations excepting the E location which shows 8-10 m/s. The southwest limb of the Bay polygon had wind speeds greater than 10 m/s for a longer time.

Fig. 4 shows the frequency distribution of vapour pressure gradient at all the locations for all the phases. During Phase I the spread at each location is higher than that of Phase II A. During Phase I the maximum frequency associated with larger values of vapour pressure gradient at S & W locations compared with the other two locations indicates a very clear horizontal gradient from southwest to northeast. In other words, vapour pressure gradient is getting diminished downstream flow. During Phase IIA on the whole there is a shift towards lower side of the spectrum at all the four locations indicating further increase in the water content of the atmosphere. The maximum frequency with larger values is now associated with S & E locations. Values greater than and equal to 10 mb occurred on very few occasions. During Phase II B the spread is high at E & W locations compared to the other two locations. The larger vapour pressure gradient values occurred more frequently at S & E locations. Here the gradient is observed diminishing from southeast limb to northwest limb of the polygon. During Phase III over northern Bay of Bengal the vapour pressure gradient values are weak compared to the corresponding ones of Arabian Sea.

Fig. 5 shows the variation of daily averaged marine meteorological parameters at the four corners of the polygon during Phase I. The surface pressure pattern at all the locations resembles very much with each other with small differences in their magnitudes. A prominent fall from 7 to 10 June at N & E locations and from 8 to 11 June at W location is due to the intensification of a well marked trough of low into a cyclonic storm known as the onset vortex over the east central Arabian Sea. A time lag of one day in the occurrence of the minimum pressure at E & W locations can be noticed on account of westward propagation of the storm. Of all the locations the N location recorded the lowest pressure of 1000 mb on 10th due to the proximity of the system to this location. On 15th another weak dip is also noticed at all the locations. Winds as high as 16 m/s at N & W locations and 15 m/s at E & S locations on 10th are associated with this severe cyclonic storm. In the entire phase the lowest daily wind speeds observed are 8 m/s at N & E locations and 6 m/s at S location and 12 m/s at W location. The average for the whole phase is highest at W location with a value of 11.2 m/s. Sea *minus* air temperature (SMA) shows violent fluctuations during the disturbed period at all the locations. The averages for the whole phase are positive at all the locations with the maximum value of 0.7 deg. C at E location and a minimum value of 0.3 deg. C at W location. A steep fall of 3 deg. C in SMA during

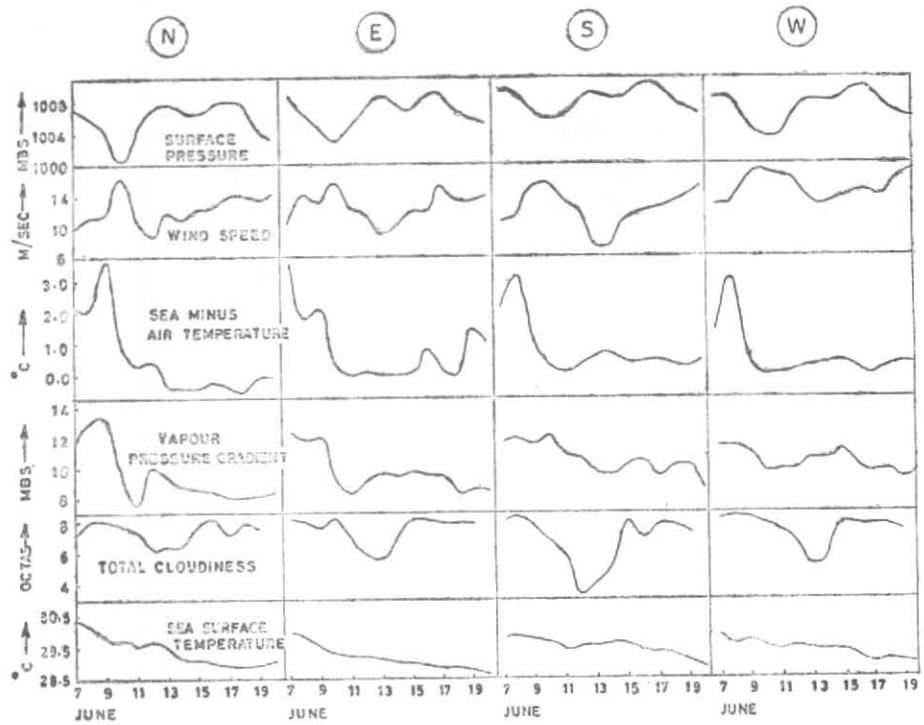

Fig. 5. Variation of daily averaged marine meteorological parameters during Phase I

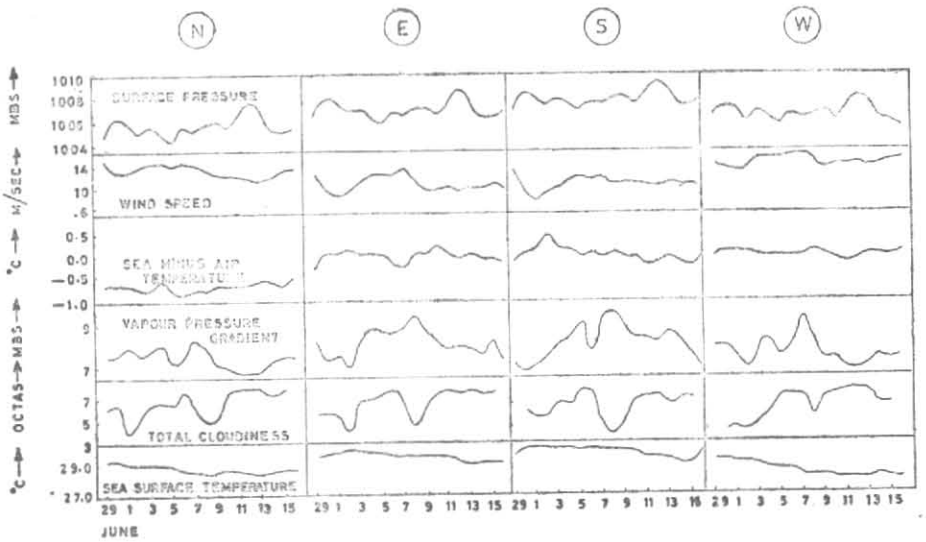

Fig. 6. Variation of daily averaged marine met. parameters for Phase IIA

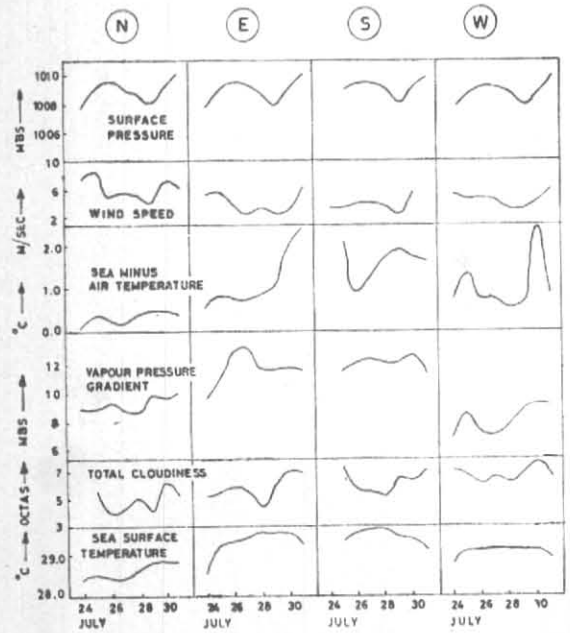

Fig. 7. Daily variation of marine meteorologica parameters in equatorial Indian Ocean during Phase II B

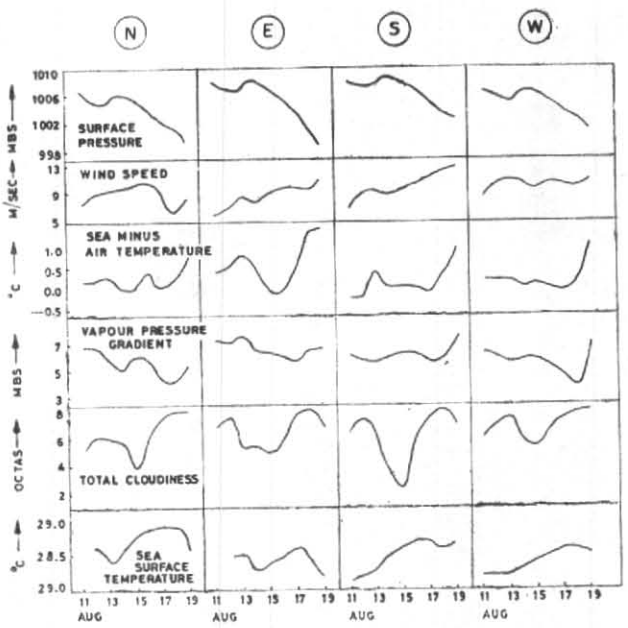

Fig. 8. Daily variation of marine meteorological parameters over northern Bay during Phase III

the disturbed period may be attributed to the corresponding fall in air temperature than that of SST caused by the storm. After the passage of the storm the SMA values oscillated around 0 deg. C at all the locations excepting at E location. Similar violent fluctuations are noticed only at N & E locations during the disturbed period in the vapour pressure gradient (VPG) curve. There is a time lag of one day between the occurrence of surface pressure minimum and VPG minimum during the disturbed weather. A marked fall of 5 mb in VPG can be noticed at the N location associated with the cyclonic storm. All the locations show a decreasing trend from the beginning to the end of the phase due to increasing moisture content of the atmosphere. The drop is more prominent at N & E locations compared to S & W locations. Cloudiness values varied between 7 and 8 octas during the disturbed period at all the locations.

Sea surface temperature shows a steady decreasing trend at all the locations. A mild increase from 11th to 14th can also be observed due to solar heating when there is a heavy reduction in the cloud cover at the S location. Only at the N location the SST is greater than 30 deg. C during the first two days. On 7th the SST values at N, E, S & W locations are 30.3, 29.9, 29.7 & 29.7 deg. C respectively. By the end of the phase the fall in SST values are 1.0 at S & W locations and 1.3 deg. C and 1.4 deg. C at N & E locations respectively, indicating a slightly greater cooling to have occurred at N & E locations. The averages during the whole phase are greater than 29 deg. C at all the locations.

Fig. 6 shows the variation of daily averaged marine meteorological parameters for Phase II A at all the locations. The monsoon has been weak along the west coast of India till 3 July and became active with the formation of a depression at the head of Bay of Bengal which got intensified into a cyclonic storm on 5th. Monsoon has been vigorous on the following two days over Kerala, Konkan and Goa along the coast. Again on 9th monsoon has become weak over Konkan and Goa. On 13th the axis of seasonal trough over Indo-Gangetic plains shifted towards north causing the break monsoon conditions to set in. There is a well marked peak in the pressure on 12th at all the locations, one day before the onset of break conditions in the monsoon.

On the first three days a drop in the windspeed is noticed and subsequently the windfield increased in association with a disturbance over northern Bay of Bengal. Winds began to fall after the Bay system got weakened and touched the minimum speeds with the onset of break conditions around 13th. Once again the monsoon current got revived and winds showed an increasing trend during the last few days of Phase II A. From Phase I to Phase II A, the average values increased at N & W locations and decreased at E & S locations.

The averages of SMA temperatures during Phase II A are near zero indicating neutral stability of the marine boundary layer. Only N location has shown — 0.71 deg. C pointing out the stable regime. The average of VPG is around 7-9 mb at all the locations and the most conspicuous feature to be noted is a fall of about 2 mb from Phase I to Phase II A. One significant peak occurred on 7th at W location while the same is observed on 8th at E location. The total cloud cover shows similar variations at all the locations.

The SST pattern shows a steady decreasing trend being more prominent at N & W locations. The averages of N & W during the phase are also lower than the corresponding ones of E & S locations. The S location has experienced the highest SST value of all the locations. Cooling from the end of Phase I to the beginning of Phase II A is 0.9, 0.3, 0.5 and 0.7 deg. C at N, E, S & W locations respectively. During Phase II A the cooling is 0.3, 0.2 and 0.6 deg. C at N, E & W locations respectively.

Fig. 7 depicts the daily variation of marine meteorological parameters in the equatorial Indian Ocean during Phase II B. The surface pressure pattern shows similar variations at all the locations with a minimum value occurring on 29th. The windfield, quite weak compared to that of Arabian Sea monsoon regime, is less than 6 m/s at all the locations with the exception of N location. The phase average at N location is higher over the other three approximately by 1.5 m/s indicating an intensification of the monsoon current after crossing the equator. Regarding SMA temperature, the N location shows weak temperature differences while the other three show large fluctuations. These differences can be attributed to the fluctuations occurred both in SST and dry bulb caused by atmospheric processes. The prominent peaks occurred at E & W locations during the last two days are due to greater fall of dry bulb than SST.

The VPG pattern clearly shows that the S & E locations encounter higher gradients compared to N & W locations. Total cloudiness pattern clearly shows an increasing trend towards the end of the phase. In the polygon the average for the duration of the phase is highest at W location and lowest at N location. SST values are much higher at S & E locations compared to N & W locations. The average SST for the phase is highest at S location and lowest at N location. A notable feature is the strong meridional gradient in SST of 0.8 deg. C in a horizontal distance of 450 km. This is the highest gradient in all the phases observed during Monsoon-77.

Fig. 8 illustrates the daily variation of marine meteorological parameters over northern Bay of Bengal during Phase III. Throughout this phase the axis of the seasonal monsoon trough remained at the foot of the Himalayas and break conditions in the monsoon prevailed. A north-south trough along the east coast of India formed on 15 August and lasted till the end of the phase. A depression formed over north-east Bay centred at 0300 GMT on 19th within ½ deg. of 19 deg. N and 91 deg. E subsequently got intensified into a deep depression crossed Orissa coast.

The most prominent feature in the surface pressure pattern is a marked fall from 14th onwards at all the locations. This feature may be attributed to the intensification of the north-south trough along the east coast of India. Lowest values of atmospheric pressure are observed on 19th. Among the four locations N & E recorded minimum values. The wind speeds in general show a steady increase in their magnitude at all the locations and attained maxima on the last day of the phase. On the whole the average wind speed of this region is weaker than the corresponding value of Arabian Sea during the first two phases. SMA temperature values are almost positive throughout indicating the unstable nature of surface atmospheric boundary layer. All the four locations show an increasing trend on the last three days pointing out the growing instability of the atmosphere leading to the formation of a disturbance. The rise is most prominent at E which is the nearest location to the depression which formed later. VPG curves at all the locations show a decreasing trend throughout, with the exception at the S location. The average VPG values at N & W locations are of similar magnitude and as of S & E locations, the former set having lower values. The total cloudiness values at all the locations show a double maxima at the beginning and end of the phase with a minima in between. From 15th onwards the rise is seen at all the locations indicating a marked convergence of water vapour associated with pre-depression conditions. The averages of SST for the phase do not show much differences at the four locations indicating near homogeneous waters in the northern Bay. But the N location is slightly warmer than the other three by about 0.25 deg. C. Excepting the E location all the remaining three show an increasing trend and peak values reached just before the formation of the monsoon depression. The period of

increase for SST roughly corresponds to the period of minimum cloudiness during the middle of the phase, thus pointing out the important role of solar heating of the surface waters. The larger SST values during the later half of the phase being greater than 28.5 deg. C might have had a contribution to the genesis of the monsoon depression.

Figs. 9 and 10 show the daily march of surface heat budget components for all the three phases at all the locations. During Phase I the net radiation (Q_N) closely followed the total cloud cover with minor deviations. The broad pattern at all the locations resembles with each other. The lower values on the first few days and around 16th of the Phase I are mainly due to large cloud cover associated with a cyclonic storm and a trough of low over east central Arabian Sea off west coast of India respectively. The latter feature is more prominent at the E location on 16th where even weak negative values can be seen. On the whole the Q_N values show 3 to 4-day epochs of high and low values alternatively. During fair weather the values are more than double the corresponding ones of disturbed weather. The average during the phase is highest at W location and lowest at E location with a difference of 100 cal/day. The latent heat exchange (Q_E) is higher during the beginning and ending days and is lower in between. Highest values of Q_E occurred on 8th, 9th and 10th at E, N & W locations respectively due to the westward moving onset vortex system north of the polygon. The evaporative losses are around 800 cal/day at N & E locations, and around 900 cal/day at W & S locations. It is interesting to note the higher losses occurred at the farther locations from the track of the storm. The Q_E curves broadly resemble with the cloudiness curves probably indicating major role played by the local evaporation in the cloud formation in this area. The average Q_E during the phase is higher at W location (737 cal/day) by approximately 100 cal/day over the other three. The fluctuations are more violent at the S location and less violent at W location as a result of the stronger variability of wind speed and vapour pressure gradient at the former. The sensible heat exchange (Q_S) values are always near zero excepting for the first two days due to the reduction of air temperature caused by cloudiness in association with the cyclonic storm. All the four locations show Q_S slightly more than 100 cal/day on different days only during the passage of the storm. On an average the E location lost 30 cal/day which is slightly more than double the values of N & W locations.

The net heat gain (Q) follows the resultant pattern of both Q_N, the main source of energy input and Q_E the main sink of energy. All the locations show large negative values of Q during the entire phase excepting the S location which shows positive values during the middle of the phase in association with fair weather. This shows that the polygon area is acting as energy source to the monsoonal atmosphere throughout this phase. The Q is higher at W & E locations and lower at S location. The highest Q at all the locations during the first few days in association of the severe cyclonic storm is around 750 cal/day which is roughly twice the average value of the phase.

During Phase IIA the Q_N values are greater than the corresponding values of Phase I at all the locations. The average Q_N during this phase is higher by 100 cal/day over Phase I average. During this phase all the locations experienced a decreasing trend in Q_N values due to an increasing trend in the cloudiness. The maximum value is seen at the S location which is greater than that of N location by 100 cal/day.

On an average, from Phase I to Phase II A, Q_E values have gone down by about 150 cal/day at W, S & E locations while the N location experienced only marginal reduction of 50 cal/day. During this phase also, highest Q_E values continued to occur at the W location as in Phase I. The northwest limb of the polygon lost around 100 cal/day higher than the corresponding value of southeast limb. Monsoon has been weak along the southwest coast of India from 29 June to 2 July and became active from 3rd onwards. The dip in the first four days in the Q_E values at all the four locations is quite evident. From 3rd onwards the quasi-permanent trough off the west coast of India became prominent in addition to the formation of a depression in northwest Bay of Bengal. The peaks in Q_E are, therefore, due to the enhanced wind strength in association with the above mentioned two systems during 4th to 7th. Once again from 9th onwards the monsoon has become weak followed by the northward shift of the seasonal monsoon trough leading to break conditions from 13th. The offshore trough has again appeared on the last three days of the phase resulting an increase in the Q_E at all the locations excepting the S location. The Q_S values are negative throughout this phase unlike those of Phase I. The average of N location during the phase is 35 cal/day while the other three locations show near zero values.

The Q values are negative throughout at all the locations excepting during the first few days. The positive peaks in Q are seen during fair weather due to an increase of Q_N when the Q_E values are also low. Higher values of

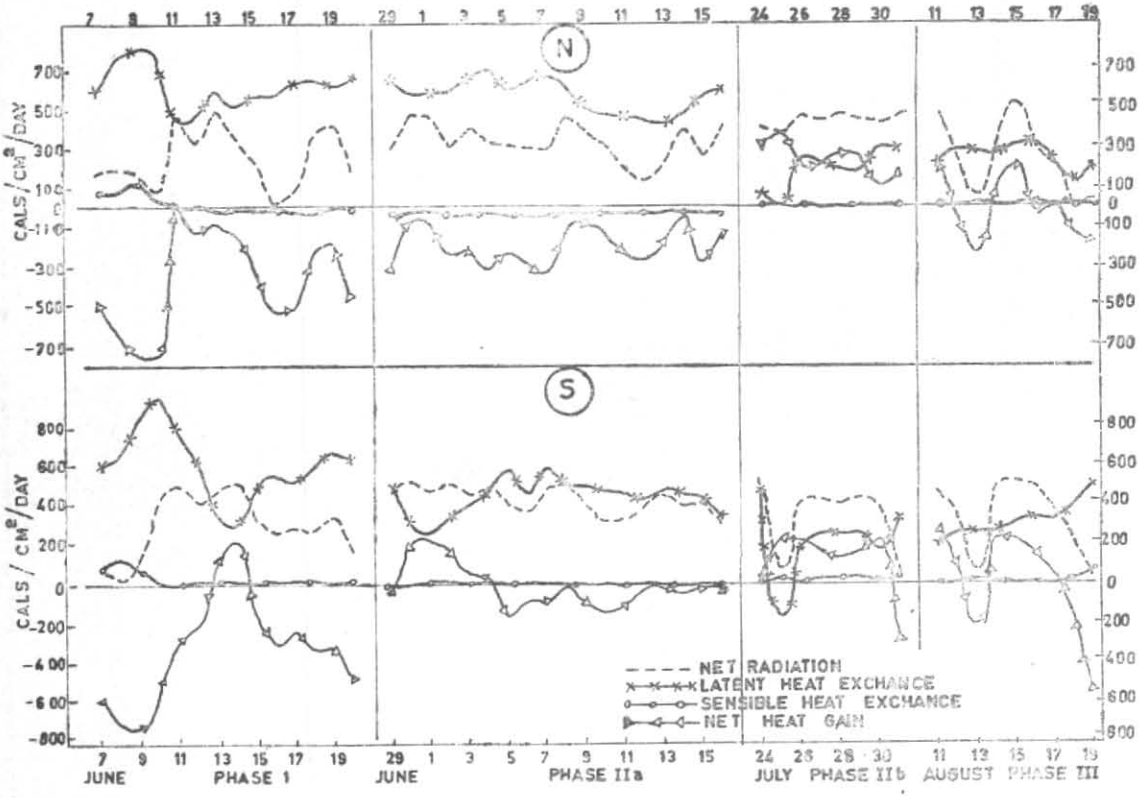

Fig. 9. March of surface heat budget components

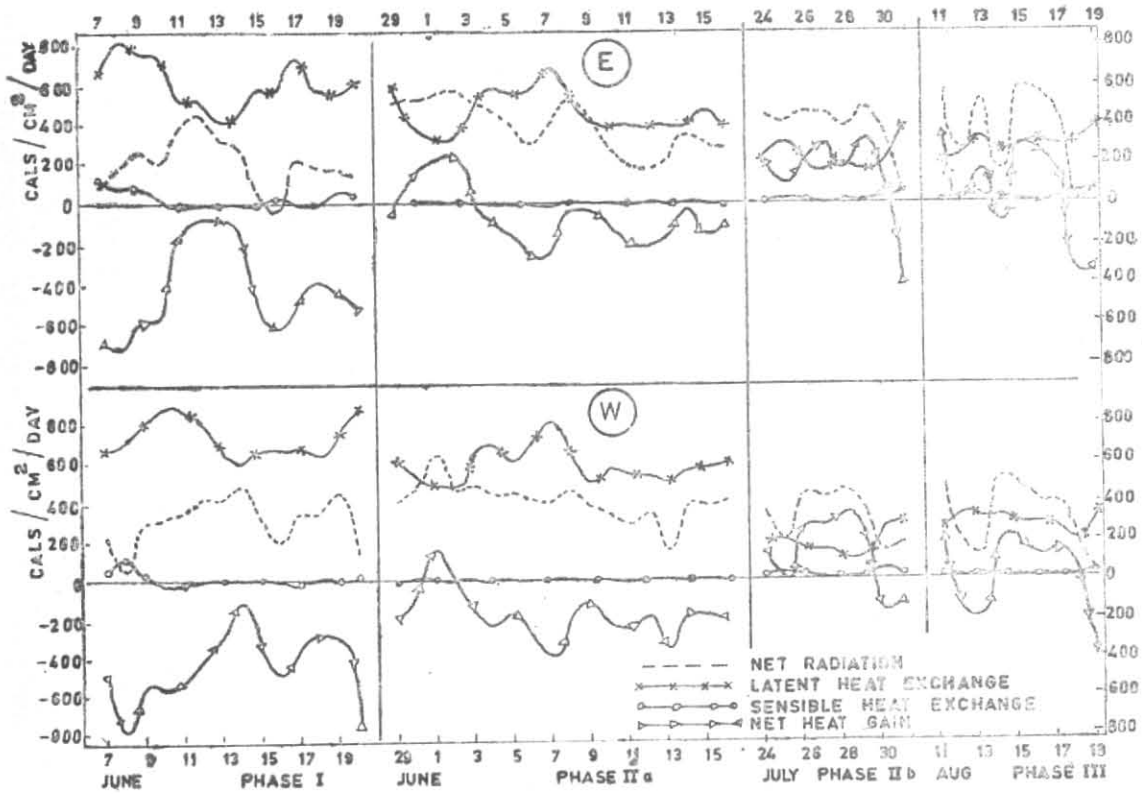

Fig. 10. March of surface heat budget components

these positive peaks are seen at S & E locations when the evaporative losses touched minima during this spell. During this fair weather period the ocean gained heat of 200 cal/day at southeast limb of the polygon. During the disturbed period from 3rd to 7th the values of Q at N&W locations are approximately—-300 cal/day. On the whole the N & W locations lost around 200 cal/day throughout the phase while the E location lost 70 cal/day and S location gained 16 cal/day. The Q values are roughly half of the corresponding losses during Phase I at N & W locations and about 1/6 th and 1/20th at E & S locations respectively.

During Phase IIB, the Q_N values are higher than the energy losses throughout the phase with an exception of few days, thus leading to energy accumulation in the upper oceanic waters. On the average the Q_N values are higher than the corresponding values during Phase I and are approximately equal to the values during Phase II A, over Arabian Sea. Over the equatorial region the N location shows the highest, Q_N value of about 440 cal/day and S & W locations show the lowest value of about 320 cal/day. This feature can be well accounted in terms of cloudiness values. Excepting the N location all the other three locations show a fall in the Q_N values from 29th associated with an increase in the cloudiness. On an average Q_E values are much lower than the corresponding ones of Phase I and Phase II A over Arabian Sea. The polygon average of Q_E is approximately about one third and half of the corresponding averages of Phase I and Phase II A respectively. Though SST values are high over this region and vapour pressure gradient is of a similar magnitude with those of Phases I and IIA, the reduction in the evaporation is mainly due to the prevailing low wind speeds at this region. Evaporation is highest at N location and lowest at W location. Q_S values are near zero throughout this phase.

The Q values are positive throughout excepting on few days when the Q_N values are low and Q_E values are high associated with the developed weather. Equatorial Indian Ocean gained energy at an average rate of 130 cal/day while the east central Arabian Sea lost energy at the rate of 390 cal/day and 140 cal/day during Phases I and IIA respectively. On an average over the equatorial Indian Ocean the N location gained highest energy and the opposite is true at the S location.

Over northern Bay of Bengal during Phase III, the marked fall in the Q_N on 13th at N, W & S locations and on 12th at E location is due to a westward moving low pressure area associated with high cloudiness. The high values on 15th are the result of clear skies after the passage of low pressure system. From 15th onwards the net radiation values began to fall again till 18th at N & E locations and 19th at W & S locations on account of the depression. The Q_E values at both S & E locations show an increasing trend throughout this phase which is quite prominent on the last three days associated with the depression over northeast Bay. On an average the Q_E over Bay of Bengal is about half of the corresponding values of Arabian Sea. The S location showed highest value and the N location showed the lowest value with a difference of 70 cal/day. At S location the highest value of 500 cal/day is observed on 19th while N location showed only 200 cal/day with the depression towards northeast of the polygon. This means that greater evaporation occurred away from the centre of the system since the atmosphere over the nearer area has already been saturated. Similar phenomenon is also observed over Arabian Sea during Phase I when the S & W locations showed greater evaporative loss when the system is nearer to N & E locations. Q_S values remained near zero throughout excepting during the end of the phase when the disturbed atmosphere gained around 50 cal/day. The Q values followed the resultant pattern of Q_N and Q_E values. On the disturbed days the values are negative due to low input of solar energy. On these days the Q is around 400 cal/day at S & W locations. During this phase on an average the net heat gain values are near zero indicating an approximate balance between the net radiation and energy losses.

5. Conclusions

(1) Variance of surface marine meteorological parameters is large during Phase I compared to that of Phase II A due to the prevailing transitory disturbed conditions associated with the monsoonal onset.

(2) The magnitudes of vapour pressure gradient and sea surface temperature are reduced from Phase I to Phase IIA while there is no corresponding change in the wind speed.

(3) Input of solar energy over the polygon area is higher during Phase IIA over Phase I by about 120 cal/day indicating that the monsoon is more vigorous at the time of its onset (Phase I) than during its sway (Phase II A) over central Arabian Sea.

(4) Greater evaporation of about 640 cal/day occurred during Phase I and during Phase IIA there is a reduction of 125 cal/day. Evaporative losses over the

polygon area are approximately double the losses occurred at two stations (Indian ships) lying in the quasi-permanent off-shore trough region along west coast of India.

(5) Throughout Phases I and II A east central Arabian Sea acted as a heat source to the monsoonal atmosphere. Over the polygon area the net heat loss from Arabian Sea during Phase I is approximately three times the corresponding loss during Phase IIA.

(6) Over equatorial Indian Ocean winds are relatively weak causing less energy loss through evaporation thus promoting energy gain at the surface.

(7) During Phase III the surface layer of Bay of Bengal is more saturated than that of Arabian Sea and the windfield is weaker over Arabian Sea during Phases I & II A. Evaporative loss from Bay of Bengal during Phase III is about half of the corresponding loss from Arabian Sea during Phase I.

(8) The energy input through solar radiation balances the energy loss over Bay of Bengal thus leading to neither diposition nor depletion of energy at the surface during Phase III.

(9) During disturbed weather conditions energy losses from the sea are double that of corresponding losses during fair weather conditions. Higher energy losses seem to have occurred from farther areas from the disturbance.

Acknowledgements

The authors wish to thank Dr. D. Srinivasan for his continuous inspiring encouragement and for the facilities provided to carry out this investigation. The authors are grateful to Prof. J. Kondo (Japan) for suggestions on the estimation of medium and high clouds. The authors wish to express their appreciation to the Project Director (Monex) for making available all the data used in the present investigation.

References

Bhumralkar, C.M., 1974, "*Relation between Air-Sea Exchange over the Arabian Sea and the fluctuations of the Western Indian Summer Monsoon*", Rand Corpn. Publications, Santha Monica, California.

Garstang, M., 1967, "Sensible and Latent Heat Exchange in low latitude synoptic scale system", *Tellus*, **19**, 3, pp. 492-508.

Kondo, J., 1975 "Air-Sea bulk transfer coefficients in diabatic conditions", *Boundary Layer Meteorology*, **9**, pp. 91-112.

Kondo, J., 1978, Personal communication.

Laevastu, T., & Ayers, E., 1966, "Numerical Synoptic Analysis of Heat Exchange and their use in Ocean thermal structure prediction", Fleet Numerical Weather Facility Technical Note 26.

Murray, F.W., 1967, "The Computation of saturated vapour pressure," *J. appl. Met.*, **6**, 1, pp. 203-204.

Pant, M.C., 1977, "Winds stress and fluxes of sensible and latent heat over the Arabian Sea during ISMEX-1973", *Indian J. Met. Hydrol. Geophys.*, **28**, 2, pp. 189-196.

Ramanadham, R., Somanadham, S.V.S. and Rao, R.R., 1981, "Heat Budget of North Indian Oceanic Surface during Monsoon-77", *Monsoon Dynamics*, Cambridge Univ. Press, pp. 491-507.

Rao, R.R., Ramam, K.V.S. and Santha Devi, M.R., 1981, "Studies on Energy Budget at selected stations over North Indian Ocean during Monsoon-77", *Monsoon Dynamics*, Cambridge Univ. Press, pp. 509-521.

Reed, R.K., 1976, " An estimation of net long wave radiation from the Oceans", *J. geophys. Res.*, **81**, 33, pp. 5793-5794.